

Intelligent Prediction of VVER-1000 Reactor Core Safety Parameter Using Neutronic and Thermo-hydraulic Coupling Models and Data mining Tools

M. Kazem Dehdashti^b

^b Department of Nuclear Engineering, School of Mechanical Engineering, Shiraz University, Shiraz 71348-51154, Iran

Abstract

The main goal of present study is to design a computational tool to predict in real-time neutronic parameters of a VVER-1000 reactor core such as axial and radial relative power distributions (RPDs) and power peaking factor (PPF) based on an artificial neural network (ANN) framework. The method utilizes ex-core neutron detector signals, some core parameters data, and a neural network to setup a real-time monitoring system for reactor's RPD and PPF predictions. To detect the hottest fuel assemblies (FAs), the radial relative power distribution in the core is monitored and then screen the axial relative power of those FAs to detect the PPF in the core. To achieve this goal, first, two hundred reactor operation states with different power density distribution are obtained by positioning the control rods in different configurations. Then a multilayer perceptron (MLP) neural network utilizing a set of data, consist of experimental and calculated data for each core state, is trained. The experimental data are core parameters such as control rods position, coolant inlet temperature, power level and signal of ex-core neutron detectors taken from Bushehr nuclear power plant (BNPP) for each core state. The reactor RPD and PPF for each corresponding state are calculated using a validated model developed in MCNPX 2.7 code. The results of this study indicates that the RPD and PPF can be determined through a neural network having as input the position of control rods, core inlet temperature, power level, coolant inlet temperature, boric acid concentration, effective days of reactor operation, and signal of ex-core detectors, accurately. Also train weighting function study illustrates that the ex-core neutron detector's signals play an important role in ANN's prediction accuracy.

Keywords: Real-time monitoring system, Relative power distribution (RPD), Power peaking factor (PPF), Artificial neural networks (ANNs), Ex-core detectors, MCNPX code

1. Introduction

An accurate prediction on the neutronic parameters of a nuclear reactor core is a major concept in its design for both economic and safety reasons. Development of economically beneficial and safe operation conditions requires more accurate, comprehensive and real-time analysis of the neutronic parameters (IAEA, 2005). In order to meet the various safety requirements imposed on the fuel pellets and fuel clad barriers such as the local power density (LPD) and the departure from nucleate boiling ratio (DNBR), which play an important role in the protection and monitoring systems, are not violated during the reactor's operation a real-time monitoring system is required (Wang et al., 2003). The changes in reactor core power distribution are usually monitored by detecting the neutron flux density via the protection system which uses in-core and ex-core neutron detectors signals. Early monitoring of the reactor power distribution and power peaking factor measurement are performed by the miniature fission chamber neutron detectors installed in the in-core instrument channels and the calculation of the power distribution is carried out with the help of a series of neutron flux data. However, utilizing the in-core neutron detectors to accurately compute the power distribution and the other real-time parameters is faced with some problems. Core size, high temperature, high pressure and some special materials proposes in the core are limitations of using in-core detectors in some cases (Bae et al., 2009). The purpose of creating an ex-core instrumentation system for advanced reactors, including VVER-1000 reactors, is to increase the safety and efficiency of nuclear power plant (NPP) operation, by increasing the response speed, reliability and accuracy of the operational monitoring system.

The main goal of this study is to predict the radial and axial RPDs and PPF in a VVER1000 reactor core using measured signals of the reactor coolant system, ex-core neutron detectors, power level, and control rods position. By studying the complex relationship between the power distribution change, core neutron flux change and ex-core neutron detector response, we find out that artificial neural networks (ANNs) could properly fit the complex nonlinear function of these aspects.

ANNs allow modelling complex systems without requiring an explicit knowledge or formulation of the relationship that exist among the variables and constitute an alternative to structured models or empirical correlations (Hassoun, 1995). ANNs have been successfully applied to different applications in nuclear engineering from nuclear reactor dynamics simulation to the PPF estimation and the 3D power distribution prediction (Pirouzmand et al., 2011; Hadad and Pirouzmand, 2007; Tanabe and Yamamoto, 1993; Nae et al., 2004; Mary et al., 2006; Montes and Francois, 2009; Xia et al., 2013). This work proposes a method, based on the artificial neural network technique to predict the radial and axial RPDs and PPF accurately in real-time. To verify the validity of this method, a series of experimental data taken from the Bushehr nuclear power plant (BNPP) are used. All of these parameters are usually deduced from the core variables such as the signals from ex-core detectors, position of control rods, power level, coolant inlet temperature, and boric acid concentration.

2. VVER-1000 Ex-Core Nuclear Measurement System

VVER-1000 reactor core can be divided into similar 60° (degree) symmetry each one contain 28 segments (FAs). As long as the neutron flux of each segment is obtained, the axial RPD of the core can be calculated in certain conditions. When the reactor core operates at hot zero power, each segment can be viewed as a neutron source and the neutron leakage from each segment is almost constant and that is monitored by ex-core neutron detectors. The escaped neutrons can cross over the surrounding segments, the reflective layer, and the pressure vessel and finally reach to the ex-core detectors. Meanwhile, the count of the detector is the superposition of the neutrons leaked from each segment. Therefore, a correspondent relationship would exist between the measured data and the neutron flux density value of each segment. In addition, for neutron flux, there is a strong correlation between each segment, especially between adjacent ones. Also the change of the neutron flux in one segment interacts neighboring segments as well as remote segments. The ex-core neutron detector is extremely sensitive to the neutron flux change of the peripheral segment. Consequently, the change of the core neutron flux distribution can be deduced from the count rate of the ex-core neutron detectors (Xia et al., 2013).

The ex-core neutron detectors of the VVER-1000 reactor together with the corresponding electronic systems can monitor the core's neutron leakage under power operation within the range of (10^{-9} to 120) % rated power. In addition, the ex-core measurement system provides some critical core parameters such as reactor period over the range of (10 to 500) seconds, reactivity, monitoring of neutron flux during start-up of reactor and reactor core loading (refuelling). Fig.1 shows the ex-core neutron detectors arrangement around the core in instrumentation and control (I&C) channels. There are provided 15 neutron detector channels in the biological shield with different measuring level. Measuring level is divided into three groups; consist of start-up, operation and source ranges. The channels 1, 6, and 12 measure the neutron leakage during the start-up and operation ranges, the channels 3, 7, and 11 are used during source range, and the channels 4, 9, 15, 2, and 13 are responsible of measurement during the source range. The detectors are located in two different vertical levels. The main task of the ex-core nuclear measurement system is to alarm timely during steady power operation and active the shutdown system when it is needed, by monitoring the neutron flux. This research addresses the RPD and PPF predictions from the ex-core measurement system in 1/6 core symmetry. Here, the signal of one neutron detector is used for the neural networks training, validation and testing (AEOI, 2007).

3. MCNPX Model

A Monte Carlo method does not solve an explicit equation like a deterministic code; it rather calculates the solutions by simulating individual particles and recording some aspects (tallies) of their average behavior. Monte Carlo codes make use of a continuous energy scale to represent the variation of the cross section data that are widely used because of their capability in modeling of complex geometries (Dunn and Shultis, 2011). MCNPX 2.7 which is a Monte Carlo based computer code and has some features such

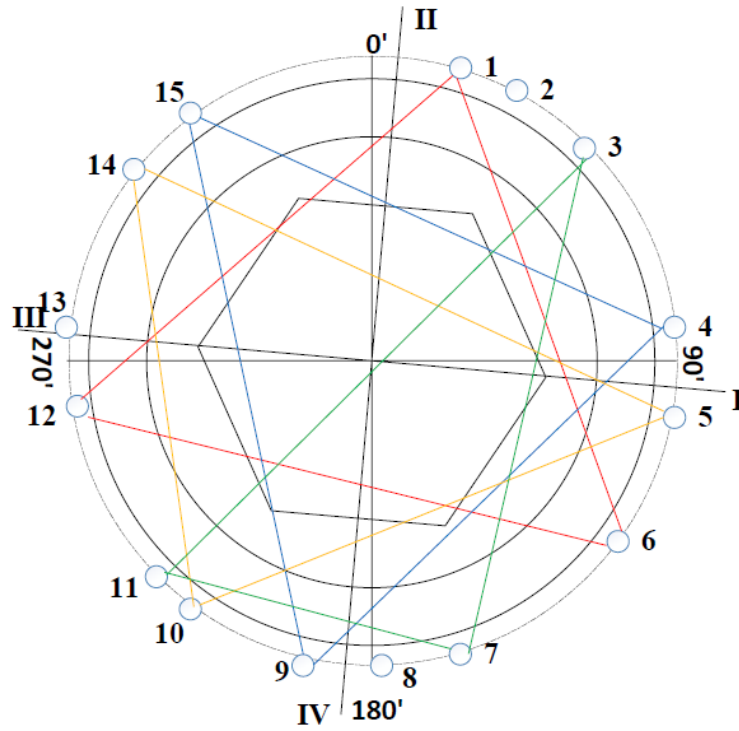


Fig. 1. Diagram of detection unit arrangement in I&C channels (AEOI, 2007)

As being general-purpose, continuous-energy, generalized-geometry, burnup calculation, and various particle transport calculation is used in this research for RPD and PPF calculations (Pelowitz, 2008).

In this study, a VVER-1000 reactor core model is designed and developed by MCNPX 2.7 code. The model contains all physical core components in real reactor operation conditions. Different tallies are considered in this model to calculate the axial and radial relative power distributions. All fuel rods (material and clad), water channels, guide channels and control rods are divided to ten axial nodes to consider the effect of coolant temperature and density distributions on the core axial relative power calculations. Axial temperature distribution for each core state is calculated using a model of VVER-1000 reactor based on Unit 1 of BNPP developed in RELAP5/MOD3.2 code consists of 4-loop primary and secondary systems with all their relevant sub-systems (Pirouzmand et al., 2014). The RPD is affected by major factors such as: the time of operation, the coolant inlet temperature, the position of control rods groups, the power level, and the boric acid concentration. Fig. 2 shows BNPP VVER-1000 core configuration including different fuel assemblies (FAs) with corresponding enrichment value at the first fuel cycle. Also, Table 1 presents the characteristics of different FA types are used at the first fuel cycle (AEOI, 2007).

The MCNPX model is validated against BNPP FSAR and neutron album data during the first fuel cycle. The calculation is carried out in the first fuel cycle for 0.00 to 293.82 days of operation with variation in the control rods position, the boric acid concentration, the power level, and the coolant inlet temperature. Also, many actual steady state and transient reactor operation states with different effective factors are applied to calculate axial and radial RPDs for each FA in ten axial nodes.

Table 2 presents some part of the MCNPX model results that are compared with BNPP neutron album (BNPPNA) data. In this table T_{eff} , T_{in} , $H10$, P , C_{bc} , K_q , K_v , N_k , and N_z are the time of reactor operation, core inlet temperature, position of control rods group 10 (percent of withdrawn length), power level, boric acid concentration, radial and axial PPFs, FA number, and core axial level, respectively.

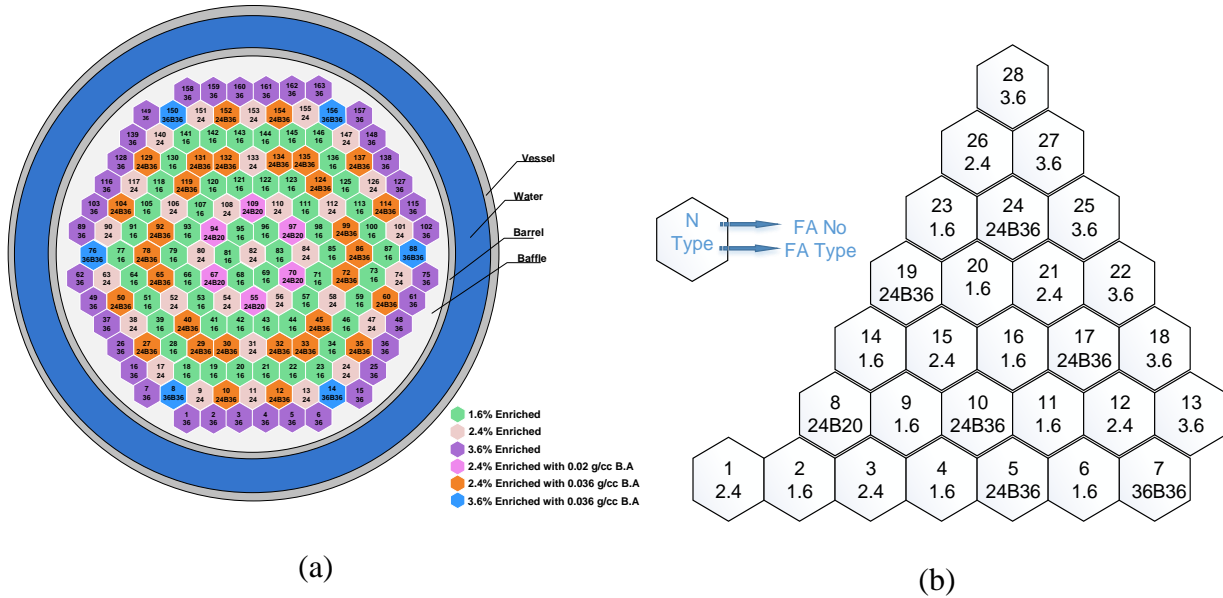


Fig. 2. VVER-1000 core configuration including different FAs in the first fuel cycle (a) whole core and (b) 1/6 core symmetry (AEOI, 2007).

Table 1. Description of FA types used in the first fuel cycle (AEOI, 2007).

FA type	Average Enrichment (U_{235} , % weight)	Number of fuel rods type 1 (% enrichment)	Number of fuel rods type 2 (% enrichment)	Number of burnable absorber rods	Boron concentration [g/cm ³]
1.6	1.6	1.6(311)	-	-	-
2.4	2.4	2.4(311)	-	-	-
3.6	3.6	3.7(245)	3.3(66)	-	-
24B20	2.4	2.4(311)	-	18	0.020
24B36	2.4	2.4(311)	-	18	0.036
36B20	3.6	3.7(245)	3.3(66)	18	0.020

Table 2. The calculated MCNPX model results compared with BNPPNA data.

T_{eff} [day]	T_{in} [°C]	H10 [%]	P [MW]	C_{bc} [g/kg]	BNPPNA (AEOI, 2004)		MCNPX Model	
					K_q [relative, N_k]	K_v [relative, N_k, N_z]	K_q [relative, N_k]	K_v [relative, N_k, N_z]
0	280.5	60	150	6.83	1.42 25	2.07 25 5	1.42 25	2.07 25 5
1	282.8	60	750	6.04	1.34 21	1.90 21 4	1.34 21	1.90 21 4
5	284.4	70	1200	5.6	1.29 21	1.78 21 5	1.29 21	1.78 21 5
10	285.5	80	1500	5.36	1.26 21	1.71 21 5	1.26 21	1.71 21 5
15	285.5	80	1500	5.3	1.26 21	1.69 21 5	1.25 21	1.67 21 5
20	288.3	80	2250	4.95	1.22 21	1.66 21 4	1.22 21	1.66 21 4
40	288.3	80	2250	4.74	1.22 1	1.60 1 5	1.22 1	1.60 1 5
60	288.3	80	2250	4.16	1.22 1	1.52 3 5	1.22 1	1.52 3 5
70	288.3	80	2700	3.93	1.24 1	1.52 3 4	1.23 1	1.50 3 4
80	291	90	3000	3.93	1.24 1	1.45 3 4	1.24 1	1.44 3 4
100	291	90	3000	3.58	1.22 3	1.39 3 3	1.21 3	1.39 3 3
120	291	90	3000	2.23	1.21 3	1.37 3 3	1.21 3	1.35 3 3
160	291	90	3000	2.51	1.19 3	1.32 3 3	1.18 3	1.32 3 3
200	291	90	3000	1.76	1.17 3	1.31 3 2	1.17 3	1.31 3 2
240	291	90	3000	1.01	1.15 3	1.31 15 2	1.15 3	1.31 15 2
260	291	90	3000	0.63	1.15 3	1.31 15 2	1.14 3	1.31 15 2
293	291	90	3000	0	1.14 3	1.30 15 2	1.14 3	1.30 15 2
293.82	291	90	3000	0	1.14 3	1.30 15 2	1.14 3	1.29 15 2

The calculated average error of MCNPX model results for all operation states given in Table 2 are shown in Fig. 3. The maximum error is less than 1.5% and 1% for axial and radial data (respectively) which is accurate enough to be used in RPD monitoring.

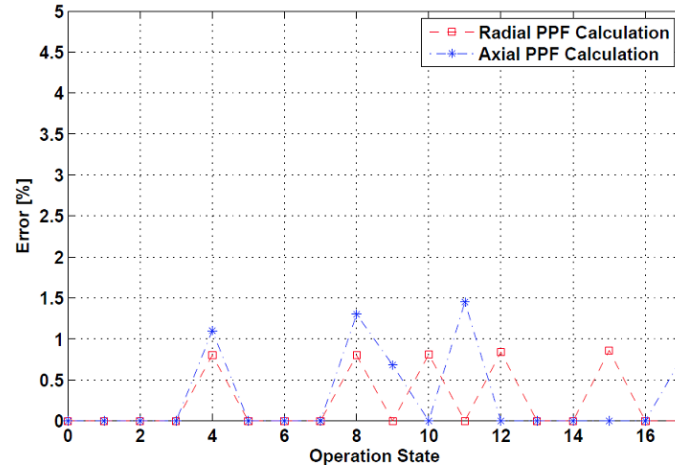
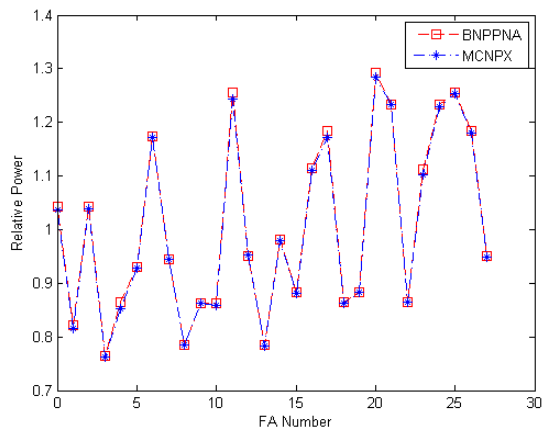


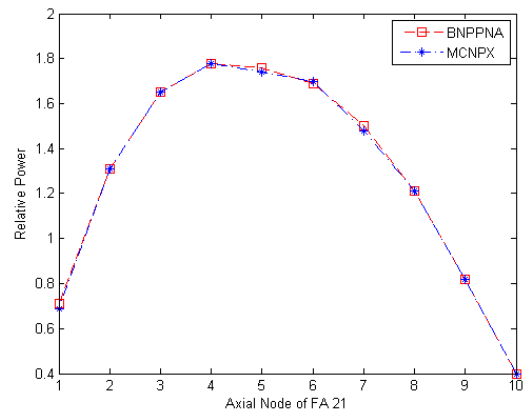
Fig. 3. Calculated average error of MCNPX model results for all operation states given in Table 2.

Table 3. One of reactor operation state investigated for MCNPX model validation

Reactor core parameter	Si_{ex} [A]	H8 [%]	H9 [%]	H10 [%]	C_{bc} [g/kg]	T_{in} [°C]	P [MW]	T_{eff} [day]
Value	8.23E-05	100	100	70	5.6	284.4	1200	5



(a)



(b)

Fig. 4. Comparison of the MCNPX model results with BNPP neutron album data (a) radial and (b) axial relative power for the operation state given in Table 3.

Also, Fig. 4 illustrates the radial and axial RPDs for an operation state with reactor core parameters given in Table 3 for further comparison. As shown there is a very good comparison between the MCNPX model results and the BNPPNA data. In this table H8, H9 and Si_{ex} are the position of control rods group 8 and 9 and the signal of ex-core neutron detector, respectively.

4. Training Data

In this research, 200 reactor operation states with different power density distributions are considered and a database is made. The database is composed of about 58000 different data containing axial and radial relative power distributions for 1/6 reactor core symmetry plus some reactor core physical parameters. The database is divided into three categories: The first subset consists of the first fuel cycle core operation states from cold zero power to hot full power with considering the change in coolant inlet temperature, power level, position of control rods group 10, boric acid concentration, magnitude of ex-core detector signal and the corresponding axial and radial RPDs and PPF calculated using the MCNPX model. The

second subset covers reactor core shutdown states including all mentioned core parameters and especially changes in reactor controlling parameters. This time, the position of three control rod groups is altered (H10 from 100 to 0, H9 from 100 to 6.6, and H8 from 100 to 66.6 percent). In the second category, the correlation between changing the position of control rods groups and the relative power magnitude is more observable. The third group is related to transient conditions, containing the irregular change in position of three control rods groups, boric acid concentration, and power level during different effective days of operation with MCNPX model output data and signal of ex-core detector for the similar reactor transient condition. Table 4 presents some of reactor core operation states in the three mentioned categories.

Table 4. Samples of reactor operation states used in training process.

Reactor core parameters								
Start-up and steady state operation	H10 [%]	H9 [%]	H8 [%]	T _{eff} [day]	T _{in} [°C]	P [MW]	C _{bc} [g/kg]	Si _{ex} [A]
	90	100	100	120	291	100	3.23	1.42E-4
	90	100	100	140	291	100	2.87	1.42E-4
	90	100	100	160	291	100	2.51	1.42E-4
	90	100	100	180	291	100	2.14	1.42E-4
	90	100	100	200	291	100	1.76	1.42E-4
	90	100	100	220	291	100	1.39	1.42E-4
	90	100	100	240	291	100	1.01	1.42E-4
	90	100	100	260	291	100	0.63	1.42E-4
	90	100	100	280	291	100	0.26	1.42E-4
	90	100	100	293.82	291	100	0	1.42E-4
Shut-down(trip in day 100)	90	100	100	100	291	100	3.58	1.42E-4
	76.6	100	100	100	289.9	90	3.58	1.40E-4
	63.3	100	100	100	288.8	80	3.58	1.40E-4
	50	100	100	100	287.7	70	3.58	1.40E-4
	36.6	96.6	100	100	286.6	60	3.58	1.40E-4
	23.3	83.3	100	100	285.5	50	3.58	1.40E-4
	16.6	76.6	100	100	284.4	40	3.58	1.40E-4
	6.6	66.6	100	100	283.3	30	3.58	1.40E-4
	0	56.6	100	100	282.2	20	3.58	1.40E-4
	0	43.3	100	100	281.1	10	3.58	1.40E-4
Transient condition	0	0	60	5	291	40	4.69	1.40E-4
	0	0	50	5	291	40	4.6	8.25E-5
	0	0	40	5	291	40	4.5	8.25E-5
	0	0	30	5	291	40	4.37	8.25E-5
	0	0	20	5	291	40	4.23	8.25E-5
	0	0	10	5	291	40	4.13	8.25E-5
	0	0	0	5	291	40	4.09	8.25E-5
	30	90	100	50	291	75	4.65	9.90E-5
	20	80	100	50	291	75	4.65	9.90E-5
	10	70	100	50	291	75	4.65	9.90E-5

5. Artificial neural networks

Artificial neural networks (ANNs) are defined as a parallel distributed processor consisting of a great number of processing elements, known as neurons, connected to each other with different connection strengths. The strength of a connection between neurons is called weight. In the beginning of the neural networks development process, these weights are initialized randomly and adjusted in a network's training process in a way that it minimizes the error between the calculated outputs and the corresponding target output values for the particular training data set, while the testing subset is used to check the performance of the developed network. There are different types of ANNs depending on their applications. Fig. 5 shows a multi-layer perceptron (MLP) neural network with three hidden layers used in this study (Hassoun, 1995).

Two hundred samples from the MCNPX model and experimental data are used to train, validate and test the networks. The relative power could be correlated to several variables. These variables and relative power distributions can be utilized for training and validating the neural networks.

According to these variables, the input vectors can be different. The first input vector includes signal of ex-core detector (Si_{ex}), position of control rods group 8, 9, and 10 (H8, H9, and H10), coolant inlet temperature (T_i), effective day of reactor operation (T_{eff}), boric acid concentration (C_{bc}) and power level (P). The outputs of network are the radial relative power for 28 FAs and axial relative power in ten axial layers for each FA.

Input file for training the network includes a matrix with 200 rows and 10 columns containing reactor core parameters and ex-core neutron detector signal for each state. Target is a 200×280 matrix containing relative power for each axial node of each FA in 1/6 core symmetry (28 FAs).

In this study MLP neural networks with one and two hidden layers and various number of neuron in each layer are investigated to choose the best network architecture. The MLP networks are model in MATLAB Neural Network Toolbox. Logsig and Purelin transformation functions are utilized and the train function in this work is trainlm which is a network training function that updates weight and bias values according to Levenberg-Marquardt optimization (MathWorks, 2014). Seventy percent of data sets is used for training, 15% is applied for validation and the remaining 15% is employed to test the proposed networks. The performance of networks to estimate the RPD is summarized in Table 5. This table shows the topologies

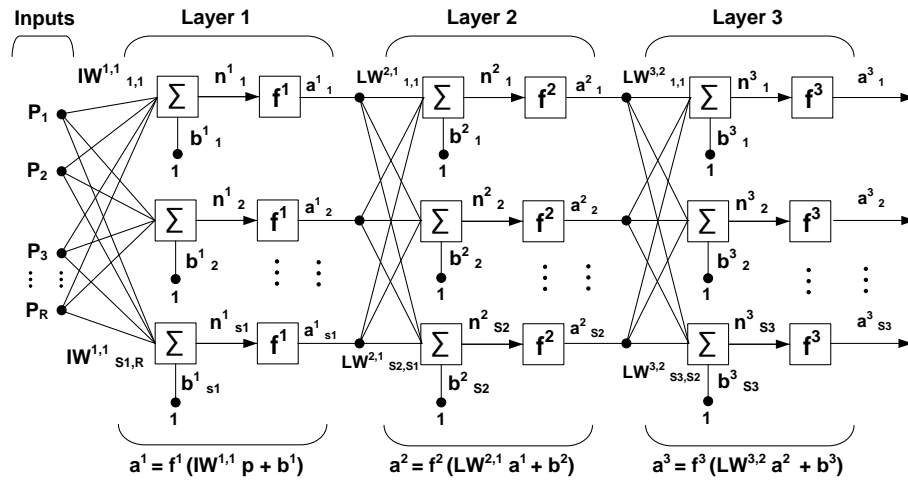


Fig. 5. Multi-layer perceptron neural network structure (Hassoun, 1995).

Table 5. Architecture and root mean square error for proposed MLP neural networks

	Architecture (# of neuron in each hidden layer)	MSE	Regression fraction
Case 1	(5)	0.0111	0.9374
Case 2	(3,10)	0.0095	0.9337
Case 3	(7,10)	0.0052	0.9276
Case 4	(9,10)	0.0009	0.9827
Case 5	(13,10)	0.0029	0.9789

And the calculated mean square error (MSE) during the training process. For the MLP neural networks, the average MSE is 0.00592. The minimum MSE is 0.000923 which is for case 4, therefore for further investigation case 4 is chosen.

The chosen MPL neural network (Case 4) contains 10 and 9 neurons in hidden layers. The magnitude of error for training, validation and testing are 0.000923, 0.0081, and 0.00981, respectively. Fig. 6 shows the aggregation of network's error in the training, validation and testing processes. The error aggregation is observed to occur around the minimum error which is a criterion for a neural network with efficient performance. The best performance of network takes place in 14 epochs as illustrated in Fig. 6.

Another step in validating the network is to create a regression plot which shows the relationship between the outputs of the network and the targets. If the training were perfect, the network outputs and the targets would be exactly equal, but the relationship is rarely perfect in practice. For Case 4 MPL network, we create a regression plot as shown in Fig. 7 that represent the regression plot for total data (training, validation and testing). The solid line represents the best fit linear regression line between outputs and targets. The R value is an indication of the relationship between the outputs and targets. If $R = 1$, this indicates that there is an exact linear relationship between outputs and targets. If R is close to zero, then there is no linear relationship between outputs and targets. In our case, the training data indicates a good fit. The validation and test results also show R values that is greater than 0.99.

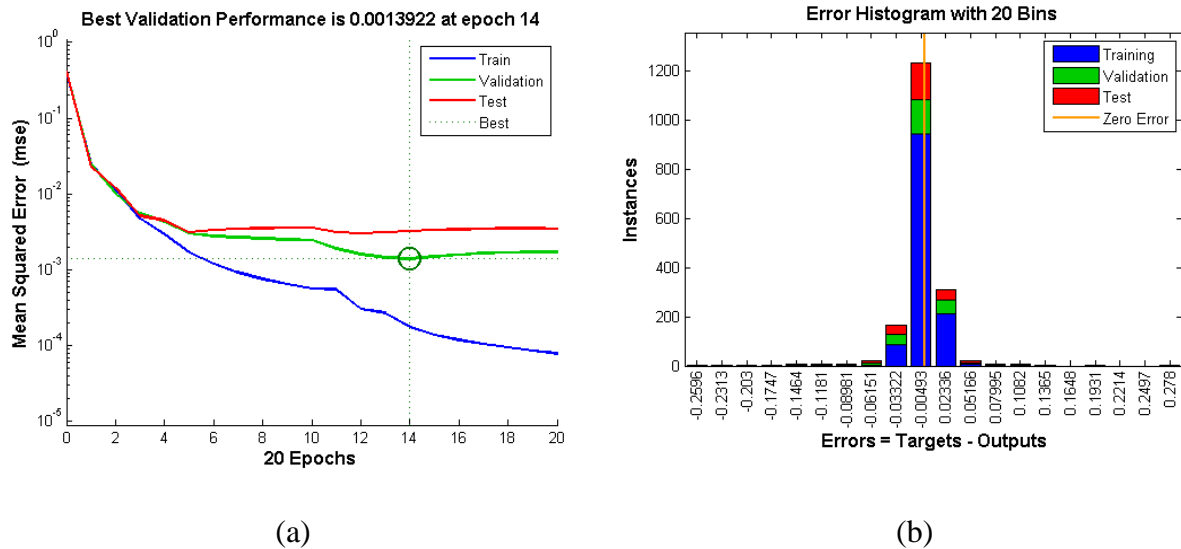


Fig. 6. The performance of MPL network during training, validation, and testing processes: (a) MSE (b) error aggregation.

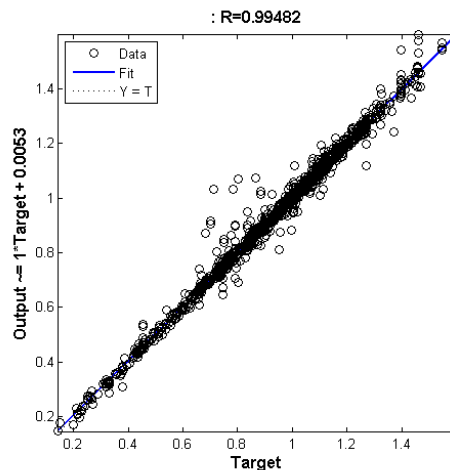


Fig 7. Regression plot for total data

As mentioned before different network's input vectors could be considered based on the number of selected core parameters. Investigation of different core parameters used in training process shows that the neutron flux change is extremely sensitive to the position of control rods groups and ex-core neutron detector signal. Therefore, in the following to express the importance of ex-core neutron detector signal's role in network's response, the ex-core signal is omitted from all input data in network's training process. The MSE value and error aggregation plots reveal that the network's performance is getting worst (Fig. 8). Also the network's regression fraction reduces to 0.92. Furthermore, as shown in Fig. 9, the network's output (RPD) illustrates a shift in maximum of axial relative power estimation in comparison with the previous network having the ex-core detector signal as an input.

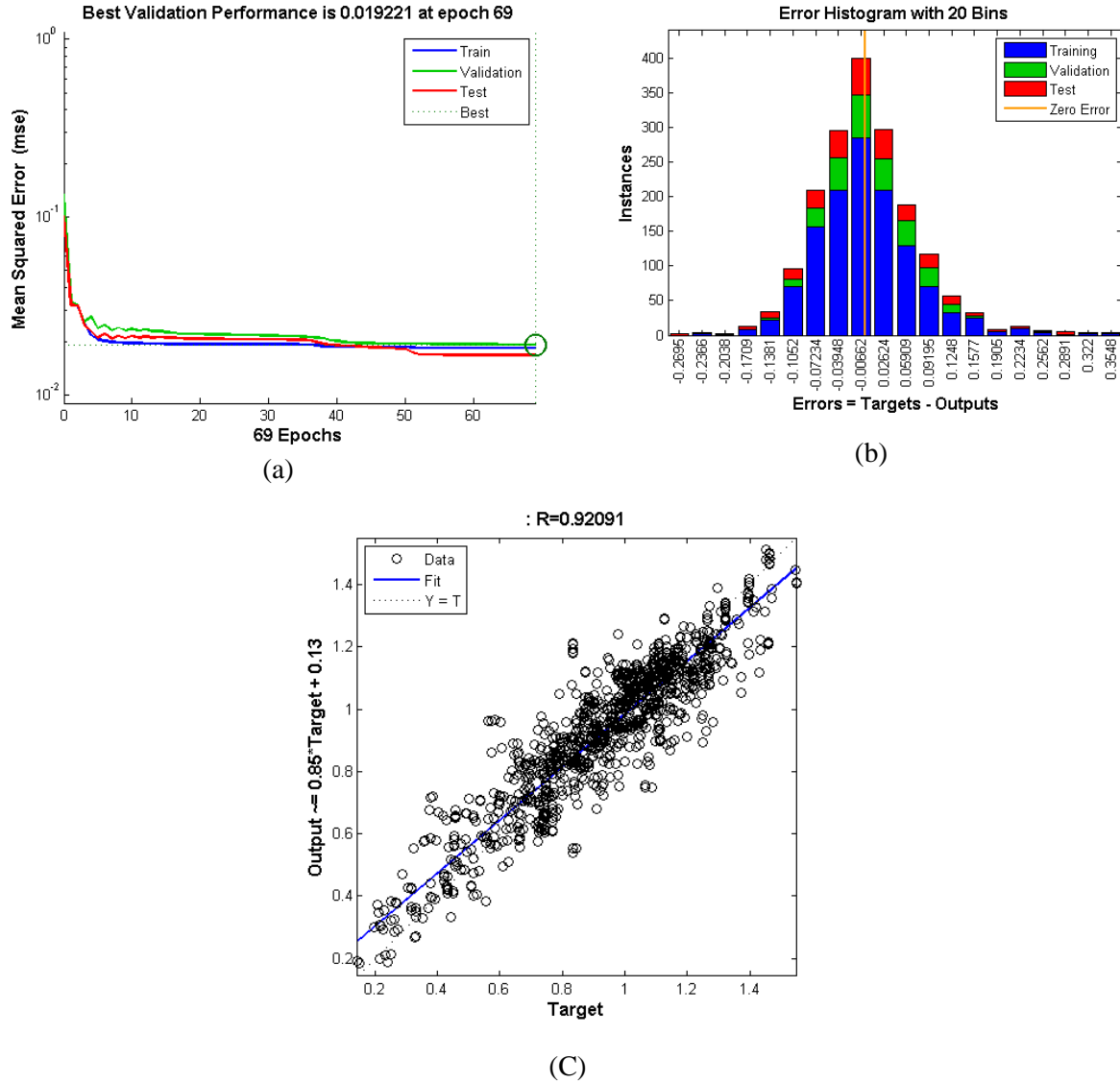


Fig. 8 The performance of MPL network after omitting the ex-core detector signal from the input vector: (a) MSE (b) Error aggregation (c) Regression plot for total data.

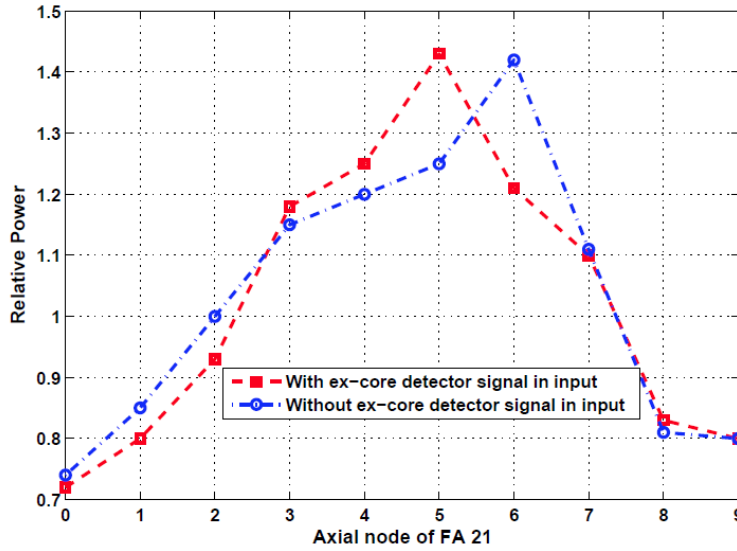


Fig. 9. Axial relative power estimation using the MLP network with ex-core detector signal compared to the same network but without ex-core detector signal in input vector.

6. ANN prediction results

In this section the MLP network's real-time prediction of relative power distribution and power peaking factor and a comparison with the BNPPNA data are discussed for five core states presented in Table 6 which are not used in training, validation, and testing processes.

Table 7 present the RPD prediction in 1/6 core by ANN compared to BNPPNA data for Case 1 core operation state given in Table 6. The PPF is occurred in the fifth node of FA number 21 where the neural network predicts the value of power peaking factor with 0.56% error.

These data are also plotted in Figs. 10 (a) and (b) for graphical comparison. Fig. 10 (a) illustrates the radial RPD prediction for 1/6 core symmetry (28 FAs) compared to BNPPNA data. Also, Fig. 10 (b) shows the axial RPD prediction in FA number 21 where the PPF is occurred.

Same data as Table 6 but for Case 2 is presented in Table 7. In this case the PPF is occurred in the third node of FA number 27 where the neural network predicts the value of PPF with 0.6% error. Fig. 11 (a) illustrates the radial RPD prediction for 1/6 core symmetry compared to BNPPNA data. Also, Fig. 11 (b) shows the axial RPD prediction in FA number 27 where the PPF is occurred.

The error values in radial RPD prediction by ANN for each FA in 1/6 core are shown in Fig. 12 for all cases given in Table 6. The average error for Case 1 to 5 are 0.99%, 0.22%, 0.14%, 0.93% and 0.36% , respectively.

Table 6. Five reactor operation states used for the network performance evaluation of axial and radial RPDs prediction

Core parameter	Si _{ex} [A]	H8 [%]	H9 [%]	H10 [%]	C _{bc} [g/kg]	Ti [°C]	P [MW]	T _{eff} [day]
Case 1	8.23E-05	100	100	70	5.6	284.4	1200	5
Case 2	8.25E-05	30	90	0	4.99	284.4	1200	5
Case 3	3.43E-04	100	70	10	----	284.4	1500	200
Case 4	3.85E-04	100	66.6	6.6	0	283.3	1250	100
Case 5	2.65E-03	10	80	20	----	281.0	500	300

Table 7. RPD prediction by ANN compared to BNPPNA data for Case 1 given in Table 6

		Axial node's number in each FA										
			1	2	3	4	5	6	7	8	9	10
FA's number	1	BNPPNA	0.56	1.02	1.30	1.43	1.45	1.39	1.24	1.00	0.71	0.35
		ANN	0.55	1.00	1.30	1.43	1.44	1.39	1.23	1.00	0.71	0.34
	2	BNPPNA	0.45	0.80	1.02	1.13	1.15	1.10	0.98	0.79	0.55	0.28
		ANN	0.43	0.80	1.02	1.13	1.15	1.09	0.98	0.79	0.55	0.25
	3	BNPPNA	0.57	1.03	1.31	1.44	1.46	1.39	1.23	0.97	0.67	0.33
		ANN	0.55	1.03	1.31	1.43	1.46	1.39	1.21	0.97	0.67	0.30
	4	BNPPNA	0.42	0.75	0.95	1.05	1.07	1.02	0.89	0.70	0.48	0.24
		ANN	0.41	0.75	0.93	1.04	1.07	1.02	0.83	0.70	0.48	0.22
	5	BNPPNA	0.48	0.86	1.09	1.19	1.21	1.15	1.02	0.81	0.57	0.28
		ANN	0.44	0.86	1.07	1.19	1.20	1.13	1.02	0.80	0.57	0.27
	6	BNPPNA	0.51	0.92	1.15	1.26	1.27	1.20	1.08	0.88	0.63	0.32
		ANN	0.53	0.90	1.15	1.24	1.27	1.17	1.08	0.88	0.61	0.31
	7	BNPPNA	0.64	1.18	1.48	1.60	1.60	1.51	1.35	1.12	0.81	0.39
		ANN	0.61	1.18	1.48	1.58	1.60	1.50	1.35	1.11	0.81	0.38
	8	BNPPNA	0.51	0.93	1.17	1.29	1.32	1.25	1.11	0.88	0.61	0.30
		ANN	0.50	0.93	1.14	1.29	1.31	1.25	1.11	0.87	0.60	0.30
	9	BNPPNA	0.44	0.79	1.00	1.10	1.12	1.06	0.93	0.70	0.47	0.23
		ANN	0.45	0.77	1.00	1.10	1.11	1.06	0.92	0.70	0.47	0.21
	10	BNPPNA	0.49	0.87	1.10	1.21	1.23	1.17	1.02	0.77	0.52	0.26
		ANN	0.42	0.85	1.10	1.21	1.22	1.15	1.02	0.77	0.50	0.25
	11	BNPPNA	0.48	0.86	1.09	1.19	1.20	1.14	1.01	0.82	0.58	0.29
		ANN	0.48	0.85	1.09	1.18	1.20	1.14	1.01	0.80	0.58	0.29
	12	BNPPNA	0.69	1.27	1.58	1.71	1.71	1.62	1.45	1.19	0.86	0.42
		ANN	0.69	1.24	1.58	1.70	1.71	1.62	1.45	1.19	0.85	0.40
	13	BNPPNA	0.51	0.97	1.21	1.30	1.30	1.23	1.10	0.91	0.66	0.32
		ANN	0.51	0.96	1.21	1.27	1.30	1.21	1.10	0.90	0.65	0.32
	14	BNPPNA	0.44	0.79	1.00	1.10	1.12	1.06	0.93	0.70	0.47	0.23
		ANN	0.44	0.77	1.00	1.10	1.12	1.06	0.91	0.70	0.45	0.22
	15	BNPPNA	0.58	1.05	1.32	1.45	1.47	1.39	1.15	0.75	0.44	0.21
		ANN	0.55	1.05	1.32	1.45	1.45	1.39	1.14	0.75	0.43	0.21
	16	BNPPNA	0.50	0.89	1.12	1.23	1.24	1.17	1.03	0.79	0.54	0.27
		ANN	0.52	0.89	1.12	1.23	1.24	1.15	1.03	0.77	0.54	0.25
	17	BNPPNA	0.62	1.13	1.41	1.53	1.53	1.45	1.29	1.05	0.75	0.37
		ANN	0.62	1.13	1.40	1.53	1.53	1.45	1.27	1.05	0.75	0.37
	18	BNPPNA	0.64	1.21	1.50	1.62	1.61	1.52	1.36	1.12	0.81	0.39
		ANN	0.64	1.21	1.50	1.62	1.61	1.50	1.36	1.12	0.81	0.38
	19	BNPPNA	0.49	0.87	1.10	1.21	1.23	1.17	1.02	0.77	0.52	0.26
		ANN	0.48	0.87	1.10	1.21	1.23	1.16	1.02	0.77	0.52	0.25
	20	BNPPNA	0.50	0.89	1.12	1.23	1.24	1.17	1.03	0.79	0.54	0.27
		ANN	0.50	0.84	1.12	1.23	1.24	1.16	1.03	0.79	0.54	0.26
	21	BNPPNA	0.72	1.32	1.65	1.77	1.78	1.69	1.50	1.21	0.86	0.42
		ANN	0.72	1.32	1.64	1.76	1.78	1.65	1.50	1.20	0.86	0.42
	22	BNPPNA	0.67	1.26	1.57	1.69	1.68	1.59	1.42	1.16	0.84	0.40
		ANN	0.67	1.25	1.57	1.69	1.67	1.59	1.42	1.16	0.83	0.40
	23	BNPPNA	0.48	0.86	1.09	1.19	1.20	1.14	1.01	0.82	0.58	0.29
		ANN	0.47	0.86	1.09	1.18	1.20	1.14	1.01	0.82	0.57	0.29
	24	BNPPNA	0.62	1.13	1.41	1.53	1.53	1.45	1.29	1.05	0.75	0.37
		ANN	0.60	1.13	1.41	1.53	1.53	1.44	1.29	1.05	0.75	0.36
	25	BNPPNA	0.67	1.26	1.57	1.69	1.68	1.59	1.42	1.16	0.84	0.40
		ANN	0.67	1.26	1.56	1.69	1.68	1.59	1.42	1.16	0.83	0.40
	26	BNPPNA	0.69	1.27	1.58	1.71	1.71	1.62	1.45	1.19	0.86	0.42
		ANN	0.68	1.27	1.57	1.71	1.71	1.62	1.45	1.18	0.86	0.42
	27	BNPPNA	0.64	1.21	1.50	1.62	1.61	1.52	1.36	1.12	0.81	0.39
		ANN	0.64	1.20	1.50	1.62	1.61	1.51	1.36	1.12	0.81	0.39
	28	BNPPNA	0.51	0.97	1.21	1.30	1.30	1.23	1.10	0.91	0.66	0.32
		ANN	0.50	0.95	1.20	1.30	1.30	1.22	1.10	0.91	0.66	0.32

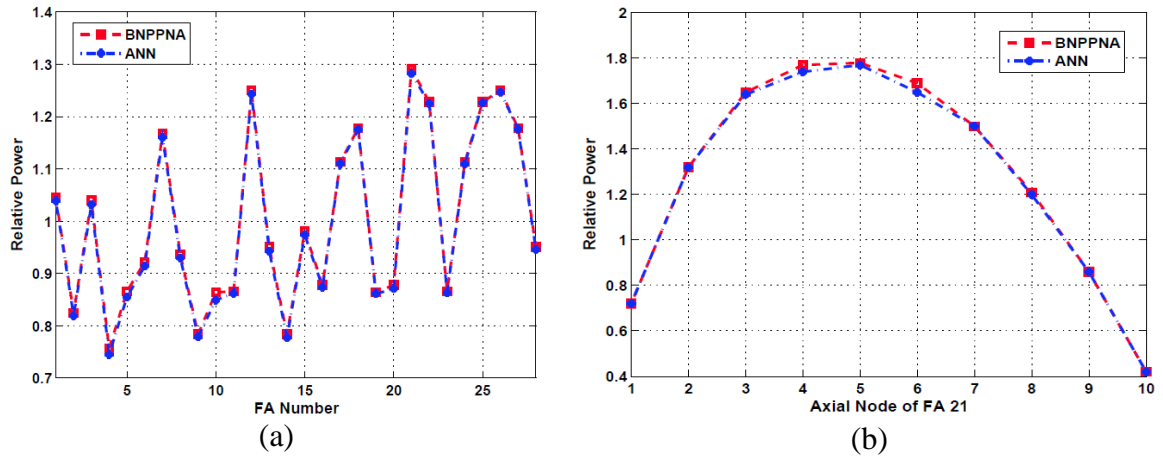


Fig10. ANN prediction results for Case 1 compared to BNPPNA data (a) radial RPD and (b) axial RPD in FA number 21.

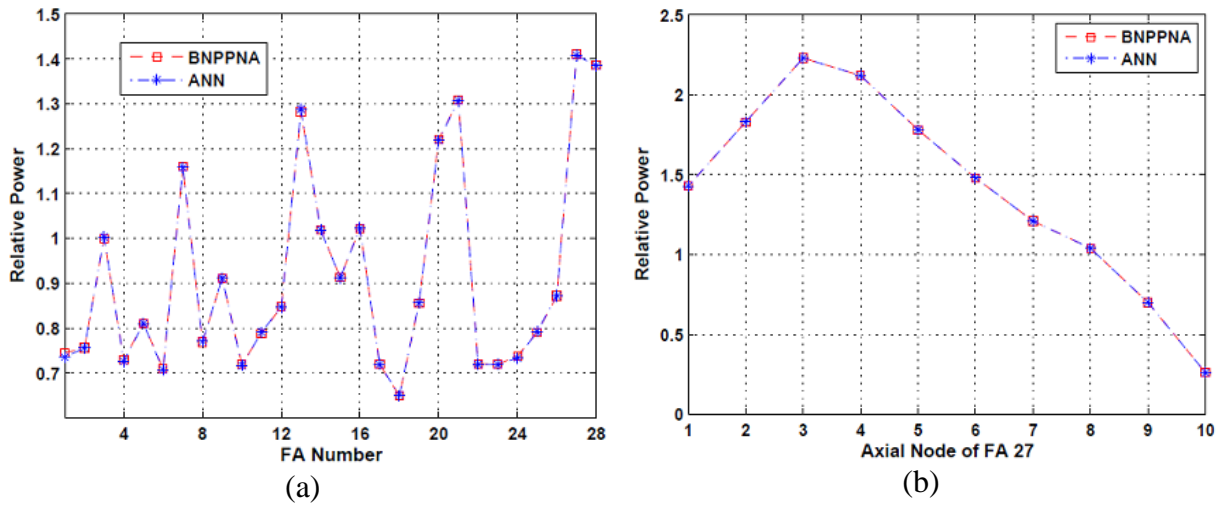


Fig11. ANN prediction results for Case 2 compared to BNPPNA data (a) radial RPD and (b) axial RPD in FA number 27.

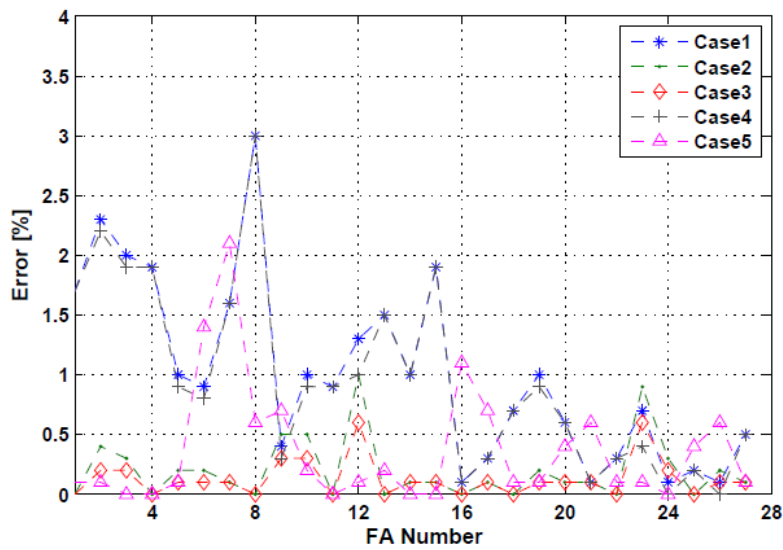


Fig12. Prediction error of radial RPD for each fuel assemblies in 1/6 core for all reactor operation states given in Table 6.

Table 8. RPD prediction by ANN compared with BNPPNA data for Case 2 given in Table 6

		Axial node's number in each FA										
			1	2	3	4	5	6	7	8	9	10
FA's number	1	BNPPNA	0.75	0.97	1.18	1.12	0.93	0.77	0.64	0.57	0.38	0.14
		ANN	0.71	0.97	1.14	1.12	0.93	0.76	0.64	0.57	0.37	0.14
	2	BNPPNA	0.77	1.01	1.20	1.15	0.93	0.77	0.64	0.59	0.35	0.15
		ANN	0.77	1.01	1.21	1.15	0.93	0.77	0.64	0.59	0.33	0.16
	3	BNPPNA	1.02	1.32	1.58	1.50	1.26	1.02	0.86	0.72	0.51	0.20
		ANN	1.06	1.32	1.58	1.50	1.26	1.02	0.85	0.72	0.51	0.21
	4	BNPPNA	0.74	0.96	1.16	1.07	0.92	0.73	0.63	0.54	0.37	0.17
		ANN	0.74	0.96	1.16	1.05	0.92	0.73	0.63	0.54	0.36	0.17
	5	BNPPNA	0.82	1.04	1.27	1.19	1.02	0.80	0.69	0.68	0.45	0.15
		ANN	0.82	1.04	1.26	1.19	1.02	0.81	0.69	0.66	0.45	0.16
	6	BNPPNA	0.72	0.93	1.12	1.06	0.89	0.71	0.61	0.55	0.36	0.14
		ANN	0.72	0.93	1.12	1.06	0.89	0.71	0.60	0.55	0.36	0.13
	7	BNPPNA	1.18	1.53	1.84	1.73	1.46	1.16	0.99	0.89	0.59	0.23
		ANN	1.18	1.52	1.84	1.73	1.46	1.16	0.99	0.88	0.59	0.23
	8	BNPPNA	0.78	1.01	1.22	1.15	0.97	0.77	0.66	0.59	0.39	0.15
		ANN	0.78	1.03	1.22	1.15	0.97	0.77	0.66	0.59	0.38	0.15
	9	BNPPNA	0.92	1.20	1.44	1.36	1.14	0.91	0.78	0.71	0.47	0.18
		ANN	0.92	1.21	1.44	1.36	1.13	0.91	0.77	0.73	0.47	0.17
	10	BNPPNA	0.73	0.95	1.14	1.07	0.91	0.72	0.62	0.55	0.37	0.14
		ANN	0.70	0.95	1.14	1.07	0.91	0.71	0.62	0.55	0.37	0.14
	11	BNPPNA	0.80	1.04	1.24	1.17	1.00	0.76	0.68	0.63	0.40	0.15
		ANN	0.81	1.03	1.24	1.17	1.02	0.76	0.68	0.63	0.42	0.15
	12	BNPPNA	0.84	1.12	1.35	1.27	1.07	0.85	0.72	0.65	0.44	0.17
		ANN	0.84	1.12	1.34	1.27	1.07	0.85	0.72	0.65	0.44	0.17
	13	BNPPNA	1.30	1.69	2.03	1.91	1.61	1.28	1.10	0.99	0.66	0.25
		ANN	1.35	1.69	2.03	1.91	1.61	1.28	1.11	0.99	0.66	0.25
	14	BNPPNA	1.03	1.34	1.61	1.53	1.29	1.02	0.87	0.79	0.52	0.19
		ANN	1.03	1.34	1.61	1.53	1.29	1.02	0.87	0.79	0.52	0.19
	15	BNPPNA	0.92	1.20	1.42	1.36	1.16	0.94	0.78	0.70	0.47	0.18
		ANN	0.92	1.20	1.42	1.36	1.16	0.94	0.78	0.69	0.47	0.18
	16	BNPPNA	1.04	1.36	1.63	1.53	1.30	1.03	0.88	0.72	0.53	0.20
		ANN	1.04	1.36	1.63	1.53	1.31	1.03	0.88	0.72	0.53	0.20
	17	BNPPNA	0.73	0.95	1.14	1.07	0.90	0.72	0.61	0.55	0.37	0.15
		ANN	0.73	0.95	1.14	1.07	0.90	0.72	0.61	0.55	0.37	0.15
	18	BNPPNA	0.61	0.82	1.04	0.99	0.83	0.66	0.57	0.50	0.34	0.13
		ANN	0.61	0.82	1.04	0.99	0.83	0.66	0.57	0.51	0.34	0.13
	19	BNPPNA	0.85	1.18	1.36	1.27	1.08	0.85	0.74	0.63	0.43	0.17
		ANN	0.85	1.18	1.36	1.27	1.08	0.85	0.74	0.63	0.43	0.17
	20	BNPPNA	1.23	1.59	1.92	1.81	1.56	1.21	1.06	0.93	0.66	0.24
		ANN	1.23	1.58	1.92	1.81	1.56	1.21	1.06	0.93	0.66	0.23
	21	BNPPNA	1.32	1.73	2.07	1.95	1.65	1.31	1.12	1.01	0.67	0.25
		ANN	1.32	1.73	2.07	1.95	1.65	1.31	1.12	1.01	0.66	0.25
	22	BNPPNA	0.73	0.95	1.14	1.07	0.91	0.72	0.62	0.55	0.37	0.14
		ANN	0.73	0.95	1.14	1.07	0.91	0.72	0.62	0.55	0.36	0.14
	23	BNPPNA	0.72	0.94	1.14	1.07	0.91	0.72	0.62	0.56	0.37	0.14
		ANN	0.72	0.94	1.14	1.07	0.91	0.72	0.62	0.56	0.37	0.14
	24	BNPPNA	0.75	0.97	1.17	1.10	0.93	0.74	0.63	0.57	0.38	0.14
		ANN	0.75	0.95	1.17	1.11	0.93	0.74	0.63	0.54	0.38	0.13
	25	BNPPNA	0.80	1.04	1.25	1.18	1.00	0.76	0.68	0.64	0.40	0.15
		ANN	0.80	1.04	1.25	1.18	1.02	0.76	0.68	0.64	0.40	0.15
	26	BNPPNA	0.85	1.14	1.36	1.28	1.06	0.86	0.73	0.56	0.44	0.44
		ANN	0.85	1.14	1.36	1.28	1.06	0.86	0.73	0.56	0.44	0.44
	27	BNPPNA	1.43	1.83	2.23	2.12	1.78	1.48	1.21	1.04	0.72	0.26
		ANN	1.43	1.83	2.23	2.12	1.78	1.48	1.21	1.04	0.70	0.26
	28	BNPPNA	1.41	1.83	2.20	2.07	1.75	1.39	1.19	1.07	0.71	0.24
		ANN	1.40	1.83	2.21	2.07	1.75	1.39	1.19	1.06	0.71	0.24

7. Conclusion

This paper introduced a new tool for RPD and PPF predictions in a VVER reactor core based on an ANN framework and a series of experimental reactor operation data that were used for network training, validation and testing to develop an accurate monitoring system which can be incorporated into the reactor protection system. The ANN technique was chosen to develop the monitoring system due to its ability in the complex and non-linear problems modelling in real-time. MLP networks with different number of

hidden layers and various number of neurons in each layer were examined for this application. Based on the results, finally, an MLP network with two hidden layers was chosen.

In this research, 200 reactor operation states with different power density distributions were considered in 1/6 core symmetry for the ANN training, validation and testing. For each state RPD and PPF values were calculated using a verified MCNPX model of BNPP. The performance of proposed ANN was evaluated by MSE calculation and regression plot that show an average MSE less than 0.6 percent and an R value greater than 0.99. Also the error aggregation was observed to occur around the minimum error which is a criterion for a neural network with efficient performance (Fig. 6(b)).

Investigation of different core parameters used in training process showed that the RPD change is extremely sensitive to the position of control rods groups and signal of ex-core neutron detector. To express the importance of ex-core neutron detector signal's role in network's response, the ex-core signal was omitted from all input data in network's training process. The MSE value and error aggregation plots revealed that the network's performance is getting worst (Fig. 8). This demonstrates the necessity of ex-core detector signals application for an accurate and reliable estimation of radial and axial RPDs and PPF using ANNs.

Finally, the ability of MLP network in real-time prediction of RPD and PPF was assessed for various practical core states which were not used in training, validation, and testing processes. The results illustrates the capability and high accuracy of the proposed MLP network in RPD and PPF predictions. As illustrated in Fig. 12 the maximum value of error is less than 3%.

In conclusion, the results of this study indicates that the RPD and PPF in a VVER-1000 reactor core can be determined accurately through an ANN having as input the position of control rods, core inlet temperature, power level, coolant inlet temperature, acid boric concentration, effective days of reactor operation, and signal of ex-core detectors.

References

- Atomic Energy Organization of Iran (AEOI), (2007), BUSHEHR Nuclear Power Plant FSAR, Chapter 7: Instrumentation and control systems (I&C)", Book1.
- Atomic Energy Organization of Iran (AEOI), (2004), Album of Neutron and physical Characteristics of The 1-st Loading of BNPP, Organization of Activities on BNPP-1Commissioning.
- Bae, I.H., Gyun, M., Lee, Y.J and Park, G.C., (2009), Estimation of The Power Peaking Factor in Nuclear Reactor Using Support Vector Machine, Nuclear Engineering and Technology, vol.41, pp.1181.
- Beale, M.H., Hagan, M.T. and Demuth, H.B., (2014), Neural Network Toolbox User's Guide, the Math Works, Inc.
- Briemeister, J.F., (2013), MCNPX "A General Monte Carlo N-Particle Transport Code, Version X.2.7, Los Alamos National Laboratory, La-13709.
- Dunn, W.L. and Shultis, J.K., (2011), Exploring Monte Carlo Methods, 1st Edition, Elsevier science.
- Hadad, K., Piroozmand, A., (2007), Application of cellular neural network (CNN) method to the nuclear reactor dynamics equations, Annals of Nuclear Energy, Vol.34, pp.406-416.
- Hassoun, M., (2003), Fundamentals of Artificial Neural Networks, a Bradford Book.
- International Atomic Energy Agency, (2005), Safety Standards Design of the Reactor Core for Nuclear Power Plants for protecting people and the environment, Design of the Reactor Core for Nuclear Power Plants
- Mary, R., Souza, G.P. and Moreira, M.L., (2006), Neural Network Correlation for Power Peaking Factor Estimation, Annals of Nuclear Energy, vol.33, pp.594-608.

- Montes, J.L. and Francois, J., (2009), Local Power Peaking Factor Estimation in Nuclear Fuel by Artificial Neural Networks, *Annals of Nuclear Energy*, Vol. 36, pp. 121-130.
- Nae, M., Jung, D.W. and Shin, S.H., (2004), Estimation of the Nuclear Power Peaking Factor Using In-core Sensor Signals, *Korean Nuclear Society*, Vol. 36, pp. 420-429.
- Pelowitz, D.B., (2008), MCNPX USER'S MANUAL, Version 2.6.0, LA-CP-07-1473.
- Pirouzmand, A., Ghasemi, A. and Faghihi, F., (2014), Safety Analysis of LBLOCA with Station Blackout for the BUSHEHR's VVER-1000 Nuclear Power Plant, Nurer2014 conference, Antalya, Turkey.
- Pirouzmand, A., Hadad, K., (2011), Cellular neural network to the spherical harmonics approximation of neutron transport equation in x-y geometry Part I: Modeling and verification for time-independent solution, *Annals of Nuclear Energy*, Vol.47, pp.225-233.
- Tanabe, A. and Yamamoto, T., (1993), Development of Neural Network for Analysis of Local Power Distributions in Bare Fuel Bundles, *Nuclear Science and Technology*, Vol. 30, pp. 804-812.
- Wang, Y., Zhengpei, F.L and Han, S., (2003), On-line Monitoring the In-Core Power Distribution by Using Ex-core Ion-Chambers, *Nuclear Engineering and Design*, Vol.225, pp.315-326.
- Xia, J., Li, B. and Liu, J., (2013), Research on intelligent monitor for 3D Power Distribution of Reactor Core, *Annals of Nuclear Energy*, Vol.73, Pages 446-454.